*Nanotechnology Perceptions*
*ISSN 1660-6795*
*www.nano-ntp.com*

# Evaluating Landslide Susceptibility in the Lower Sutlej Basin, Himachal Pradesh, India Using GIS: A Comparative Study of the Frequency Ratio and Analytical Hierarchy Process Methods

**Yashodhar P. Pathak[1], M. B. Dholakia[2], Indra Prakash[3], Girishkumar D. Jagad[4], Kashyap B. Gohil[5]**

*[1]Research Scholar, Gujarat Technological University, Ahmedabad, Gujarat-380005, India*
*[2]Director & Dean, Swarnim Institute of Technology, OPP. IFFCO, Adalaj, Kalol Highway, Gandhinagar, Gujarat, India.*
*[3]Dy. Director General (R), Geological Survey of India, Gandhinagar, India*
*[4]Asst. Professor, Civil Engineering, Vishwakarma Government Engineering College, Ahmedabad*
*[5]Asst. Professor, Civil Engineering, Shantilal Shah Engineering College, Bhavnagar*
*Email: yashodharpathak189@gmail.com*

This research presents a novel comparative analysis of Frequency Ratio (FR) and Analytical Hierarchy Process (AHP) methodologies for Landslide Susceptibility Mapping (LSM) in the Lower Sutlej Basin, Himachal Pradesh, India, revealing the superior predictive performance of the FR method through Receiver Operating Characteristic (ROC) curve evaluation. The study covers the districts of Kinnaur, Shimla, parts of Kullu, and parts of Manali. A total of 1561 landslide locations were identified, and an inventory was prepared using Google Earth and QGIS. The landslide locations were divided into two groups with a 70:30 ratio: 1093 locations (70% of 1561) were used for LSM, while the remaining 468 locations (30% of 1561) were used for validation purposes. Both FR and AHP modelling were carried out considering ten landslide conditioning factors. The FR method was selected for its statistical robustness and simplicity in handling large datasets, while AHP was chosen for its ability to incorporate expert judgment in the weighting of factors. The performance of the models was evaluated using ROC curves. The results demonstrate that FR achieved a higher Area Under the Curve (AUC) value of 0.742, compared to 0.712 for AHP, indicating superior predictive performance.

**Keywords:** Analytical Hierarchy Process; Frequency Ratio Approach; GIS; Landslide; Landslide Density; Landslide Susceptibility Modelling; ROC.

## 1. Introduction

All manuscripts Landslide Susceptibility involves predicting landslides spatially by integrating various internal factors such as geotechnical properties, geological conditions, hydrological elements, vegetation cover, and topographic attributes. The process of identifying landslide occurrences across a region based on these causative factors is termed landslide susceptibility mapping (LSM). Formally defined, LSM involves dividing the land surface into near-homogeneous zones and ranking them based on the potential and actual hazard due to landslides [1]. The evolution of LSM techniques has seen the emergence of sophisticated methods, including inventory analysis, bivariate and multivariate analyses, probabilistic frequency ratio, logistic regression, and advanced approaches such as fuzzy logic, involving the Analytical Hierarchy Process (AHP), Probabilistic Frequency Ratio, and analysis with artificial neural networks [2-12]. The qualitative approach is relatively subjective, expressing the proneness of landslides descriptively based on expert decisions [5, 8-10]. In contrast, the quantitative approach involves a numerical assessment of the relationship between slope instability and other controlling factors. Deterministic and statistical methods are two examples of the quantitative approach used in studying landslide susceptibility [3,9], [13-16]. As computational science advances, machines and different algorithms are introduced in landslide susceptibility mapping. Machine learning models, known for creating complex relationships between landslide causative factors, offer mapping based on historical data fed into the model. The availability of data, with the use of geographical information systems and remote sensing data, will further enhance the success of machine learning models. The study revealed that combining SVM with other ML models and using high-quality landslide data will result in more accurate mapping for landslide susceptibility [17]. A similar comparative analysis was conducted for popular ML methods used in landslide susceptibility mapping, focusing on improving accuracy by emphasizing Landslide Causative Factors (LCF). In the specific context of this paper, the primary focus is on a theoretical comparative study that delves into the effectiveness of two prominent methods in landslide susceptibility mapping: Frequency Ratio (FR) and Analytical Hierarchy Process (AHP). The discussion extends to their individual merits and the potential synergies they may offer, providing a nuanced perspective on their application in the field. This research aims to contribute valuable insights into the comparative analysis between FR and AHP, shedding light on their respective strengths and limitations in predicting landslide susceptibility.

## 2. Brief Overview To Frequency Ratio And Analytical Hierarchy Process

The Frequency Ratio Approach relies on establishing observed relationships between landslide occurrences and causative factors. Spatial relationships between landslide locations and explanatory variables can be determined through the Frequency Response Approach (FRA), as proposed by [6]. In this method, the frequency ratio for each subclass of individual causative factors is calculated, and the landslide susceptibility index is obtained by summing up these frequency ratio values. S. Lee conducted a comparison of Landslide Susceptibility Mapping (LSM) using the frequency ratio method and logistic regression in the Penang region of Malaysia in 2005. In a study focusing on the spatial distribution of landslides in southwest Calabria, Italy, [18] Goswami et al. (2011) utilized frequency area statistics. In their study [19]

applied the frequency ratio method to prepare LSM for the Penang region of Malaysia, achieving an accuracy of 80.03%. Additionally, they found that incorporating precipitation data in LSM improves prediction accuracy. Khan et al., 2018 used frequency ratio method for Landslide Susceptibility Mapping (LSM) and determined the most influential causative factor for landslide [21]. Fayez, Laila et al., 2018 determined Landslide Density (LD) for validation of Landslide Susceptibility Map created using Frequency Ration method [22]. Also, a comparative LSM was carried out using five different methods the frequency ratio model, AHP, the statistical index (Wi), weighting factor (Wf) methods, and the logistics regression model, incorporating a Geographical Information System (GIS) and remote sensing techniques [23].

Landslide Susceptibility Mapping (LSM) involves the consideration of numerous variables, and establishing their relationships is crucial for obtaining accurate results. Utilizing a multicriteria decision-making approach, such as the Analytical Hierarchy Process (AHP), proves highly beneficial for achieving enhanced outcomes. In the AHP methodology introduced by Saaty in 2008, four steps are involved: problem definition, goal, and alternative identification, generating pairwise comparison matrices, and determining weights for priority selection. Experts subjectively assign numbers from 1 to 9 to variables related to landslides and their importance, creating comparison matrices. Subsequently, consistency ratio and index (CR and CI) are calculated. Aafaf El Jazouli et al., 2019 used eight landslide causing factors for LSM. Weight for each factor is assigned using Analytic Hierarchy Process (AHP) depending on its influence on the landslide occurrence [20]. Also, a comparative study of FR and AHP methods were carried out and results of both were validated and compared [24].As noted from literature review in above section there are several records existing for comparative study between different landslide susceptibility mapping methods [10, 14, 23-25]. In their work [26, 27], researchers have done comparative study for the landslide susceptibility mapping using machine learning models.

## 3. Study Area

The area of interest is situated in the Indian state of Himachal Pradesh, specifically within the Sutlej Basin and its adjacent regions, which encompass the districts of Kinnaur and Shimla as well as portions of Kullu and Manali. The geographical span of the study area is from latitudes 30° 46′ 38.942″ N to 32° 05′ 9.545″ N and longitudes 76° 40′ 48.663″ E to 78° 59′ 42.463″ E. Total study area is about 13,433 sq.km. Its location map is shown in Figure 1

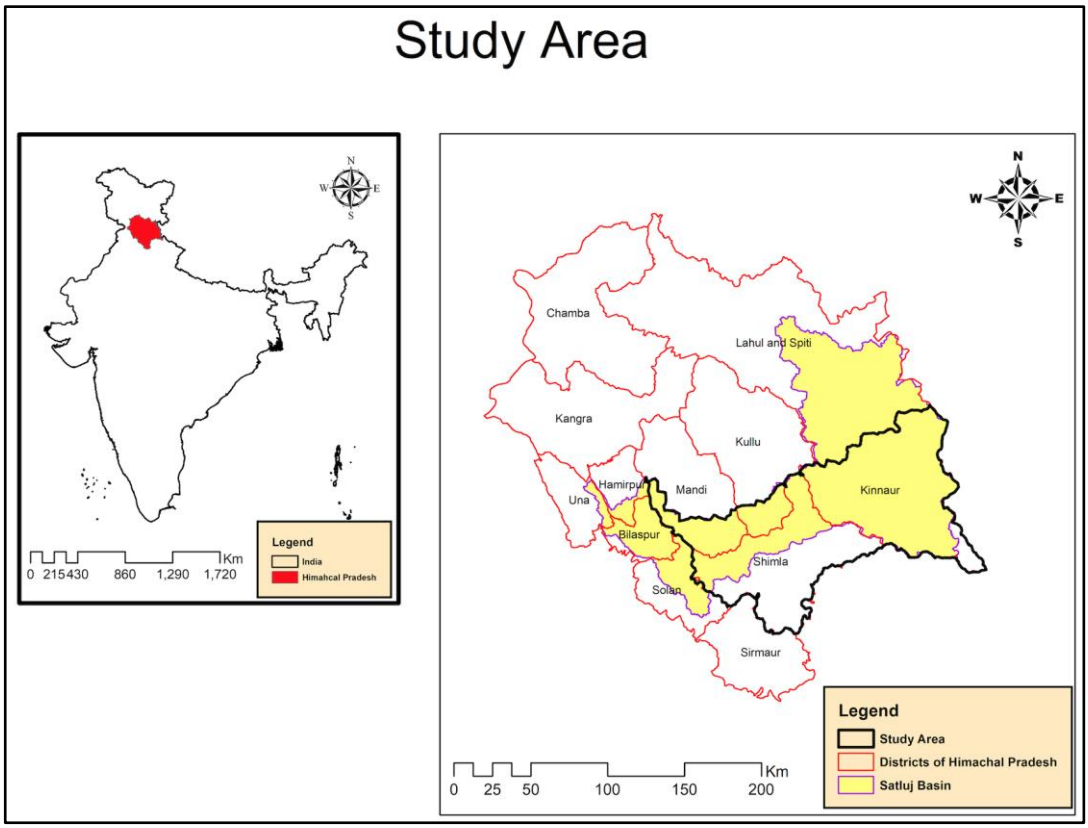


Fig. 1: Study Area

## 4. Data Collection and Analysis

Apart from landslide inventory, It is very important to select the appropriate causing factors for landslide susceptibility assessment. The landslide susceptibility modelling has required numerous data inputs, although this does not necessarily result in a high degree of accuracy while predicting landslide [28]. The correct selection of causing features depends on the type of landslide and its mechanism, study area characteristics, scale of the analysis, availability of the data, and modelling techniques to be used. Unfortunately, there is no single instruction available or recommended to select the set of causing factors for a given condition for the LSM. According to the available literature, the choice of landslide causing factors varies from one study to another. It is noticed that researchers make provision of a set of causing features which is used for LSM after adopting proper feature selection techniques [29]. The current study's feature selection process took into account a consideration of the landslide occurrences' nature in relation to the study area's geomorphology, geology, hydrology, meteorology, and human influences. Generally, the landslide causing features are divided into four groups: (i) topographical, (ii) hydrological, (iii) geological and anthropogenic [30]. For landslide analysis and modelling, we have selected 10 landslide causing factors, namely elevation, slope, curvature, distance to streams, NDVI, landcover, soil, geology, geomorphology, and distance

to roads[22]. Each factor was classified into several classes based on the standard classification for geological features except NDVI and all the topographical, hydrological and anthropogenic features along with NDVI was re-classified as per expert's knowledge method. ArcGIS and QGIS were used for the data preparation and analysis.

Data collection and analysis involves five major categories of data which is as shown below;

1. Landslide Inventory: The first crucial step in data collection and preparation is the compilation of a Landslide Inventory. This inventory serves as a foundational dataset, cataloguing information on the occurrence and location of landslides as shown in the Figure below. Total 1561 landslide locations were identified and mapped on Google Earth and inventory of the same has been prepared using QGIS. The landslide inventory map has been shown in figure 2.

2. Topographical Features: To assess the topographical characteristics of the study area, essential features such as Slope, Elevation, and Curvature are extracted from the Shuttle Radar Topography Mission (SRTM) (30m resolution) data using ArcGIS, providing valuable insights into the terrain morphology.

3. Hydrological Features: Hydrological factors play a significant role in landslide susceptibility. Distance to River, a key parameter, is derived from the SRTM data (30m) using ArcGIS. This data aids in understanding the spatial relationship between landslide occurrences and proximity to river systems.

4. Geological Features: The geological aspect involves a multifaceted approach, incorporating diverse data sources. NDVI and Landcover layers were prepared using Landsat-8 image of the study area using ArcGIS and ERDAS. The datasets like Soil type, Geology and Geomorphology are collected from various sources and raster layers of these layers were prepared. These datasets are analysed using ArcGIS and ERDAS, providing a comprehensive overview of geological conditions in the study area.

5. Anthropogenic features: Existing road network was digitised using google-earth and Arc-GIS. Also open source road network data obtained from Socioeconomic Data and Applications Centre (SEDAC) of NASA's "Earth Observing System Data and Information System (EOSDIS). It was followed by generating Distance to Road layer.

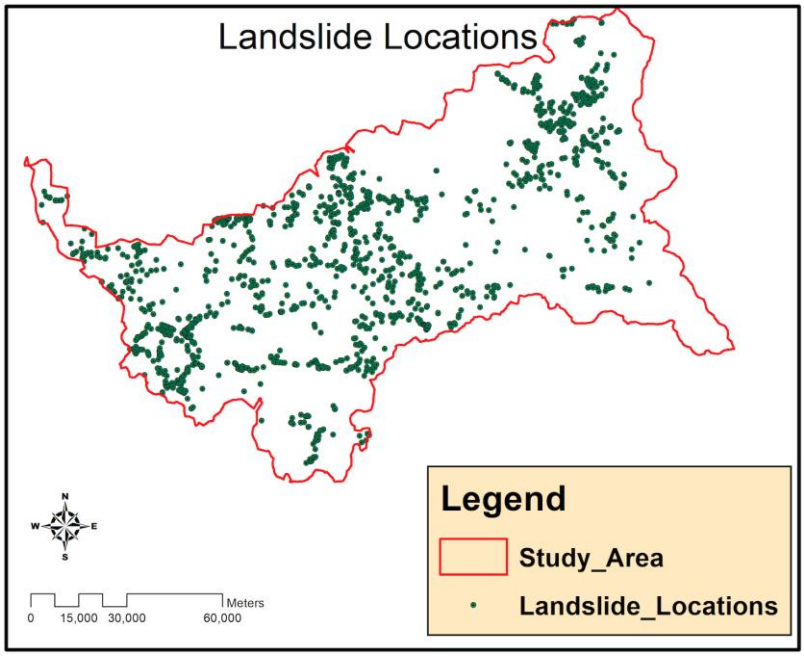


Fig. 2: Landslide Locations

The summary of various data used in the present study along with its source and tools used to generate its raster layer is shown in the table 1 below.

Table 01: Data Collection and Preparation

| Feature Name | Source (Derived from) | Tools used |
|---|---|---|
| Landslide Inventory | Geological Survey of India (GSI) - https://bhukosh.gsi.gov.in/Bhukosh/Public Landsat 8, Google Earth | ERDAS, ArcGIS |
| Topographical Features | | |
| Slope, Elevation, Curvature | Shuttle Radar Topography Mission (SRTM) (30m spatial resolution) | ArcGIS |
| Hydrological Features | | |
| Distance to River | Shuttle Radar Topography Mission (SRTM) (30m spatial resolution) | ArcGIS |
| Geological Feature | | |
| NDVI | Landsat 8 | ArcGIS |
| Landcover | Landsat 8, United States Geological Survey (USGS), Web Map Service (WMS) | ERDAS, ArcGIS |
| Soil | Food and Agriculture Organization (FAO) | ArcGIS |
| Geology, Geomorphology | Geological Survey of India (GSI) - https://bhukosh.gsi.gov.in/Bhukosh/Public | ArcGIS |
| Anthropogenic Feature | | |
| Road, Distance to Road | Socioeconomic Data and Applications Centre (SEDAC) of NASA's "Earth Observing System Data and Information System (EOSDIS)", Google Earth | ERDAS, ArcGIS |

The maps of all the ten features selected for Landslide susceptibility modelling has been shown below in Figure 3.

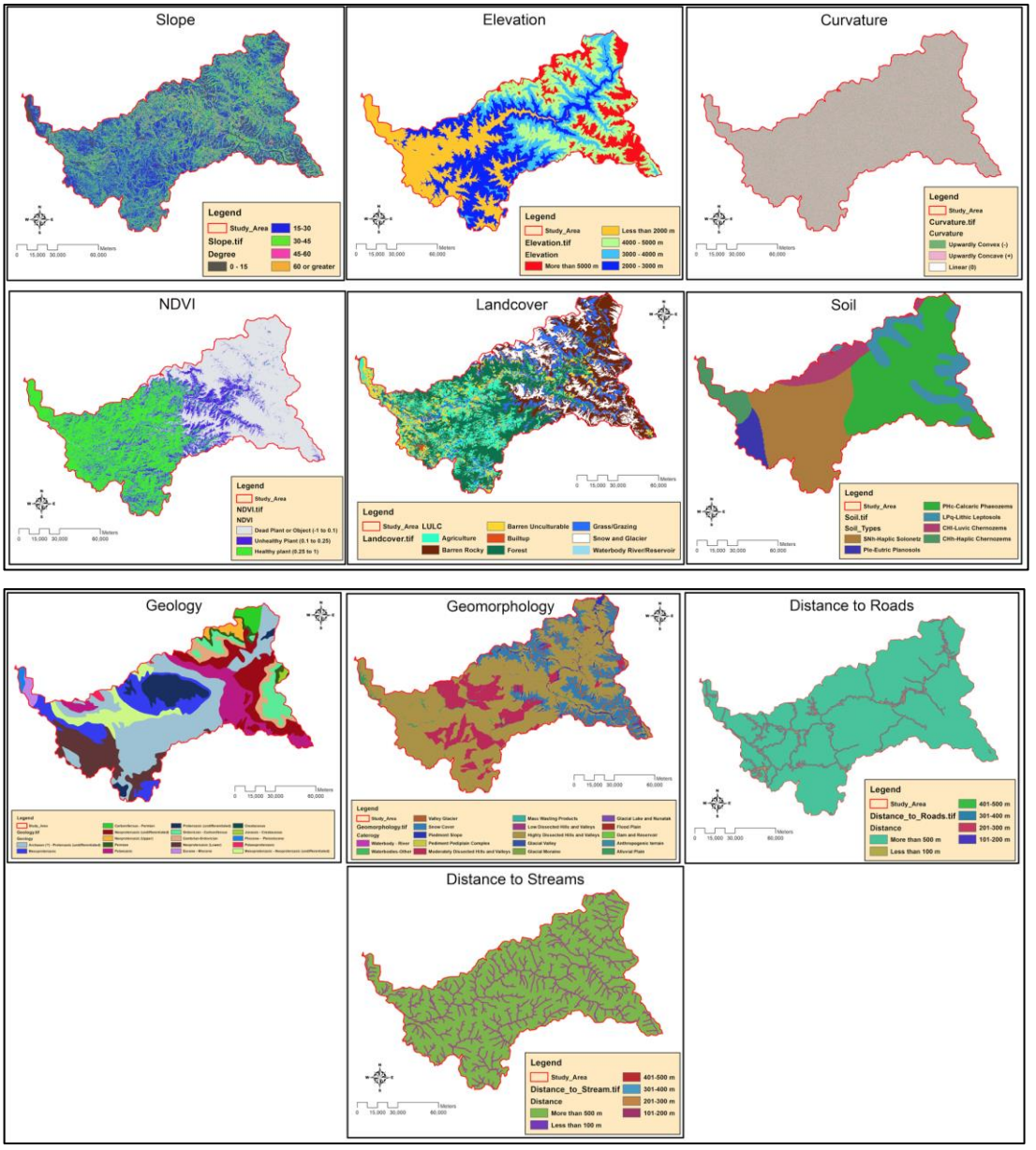


Fig. 3: Various Features Selected for Landslide Susceptibility modelling

## 5. Methodology and Analysis using Frequency Ratio

The flow of process involved in FR approach is shown in the figure 4 below.

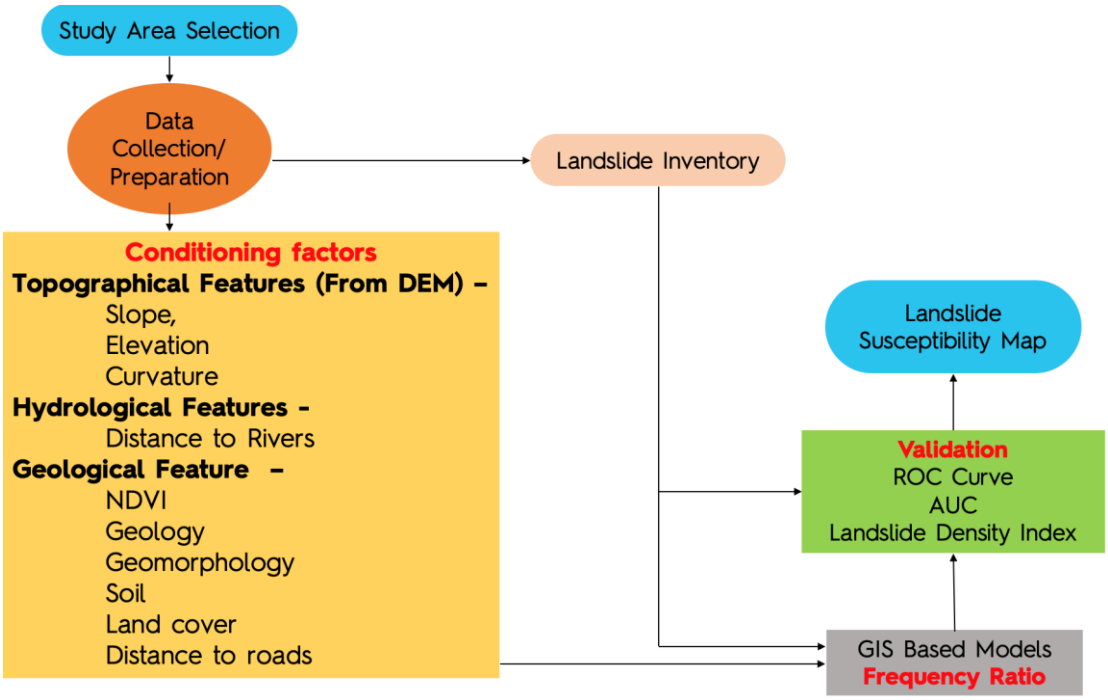


Fig. 4: Process Diagram for Frequency Ratio Approach

The methodology employed for the Frequency Ratio (FR) Method involves following sequential steps.

1) Determination of Frequency Ratio of each class of each variables by using following mathematical formula. The frequency ratio of each class of each variable have been calculated and presented in table no. 02 and figure 5 below.

$$FR = \frac{NL_i/NL_t}{NC_i/NC_t}$$

Where;

$NL_i$ : Number of landslides (LSD) in class i

$NL_t$ : Total number of landslides in the entire study area

$NC_i$ : Number of pixels of class i

$NC_t$ : Total number of pixels in the entire study area.

2) Determination of Relative Frequency (RF) by using following equation

$$RF = \frac{Frequency\ Ratio\ of\ a\ perticular\ class}{Sumation\ of\ Frequency\ Ratio\ of\ every\ class\ of\ a\ perticular\ variable}$$

RF provides insights into the proportion of landslides associated with each class of various factors.

3) Determination of prediction Rate (PR) (% influence) of each variable by using following mathematical expression.

Prediction Rate = (Maximum RF – Minimum RF) / Minimum $_{(Max.\ RF\ -Min.\ RF)}$

Prediction rate (% influence) was calculated for all the ten criteria which is shown in Table 3

4) Each class category associated with factors contributing to landslides is assigned a Relative Frequency (RF). Following this assignment, reclassification of each layer is undertaken based on the designated Relative Frequency values.

5) The subsequent step entails the generation of the Landslide Susceptibility Index (LSI) map, achieved by summing the products derived from the Relative Frequency and Prediction Rate across all layers.

Table 02: Calculation of Frequency Ratio, Relative Frequency and Prediction Rate

| Sr. No | Layer | Category | Nos. Of LSD (NLi) | LSD % | Area (No. Of Pixel) NCi | Area % | FR (FRi) | RF | RF% | RF (INT) | Min (RF) | Max (RF) | Max RF - Min RF | Min (Max RF – Min RF) | PR |
|---|---|---|---|---|---|---|---|---|---|---|---|---|---|---|---|
| 1 | Slope | 0 - 15 | 41 | 3.75 | 1837 | 12. | 0.30 | 0.05 | 5.10 | 5.00 | | | | | |
| | | 15-30 | 378 | 34.5 | 6584 | 44. | 0.78 | 0.13 | 13.13 | 13.00 | | | | | |
| | | 30-45 | 582 | 53.2 | 5733 | 38. | 1.39 | 0.23 | 23.21 | 23.00 | | | | | |
| | | 45-60 | 90 | 8.23 | 7550 | 5.0 | 1.63 | 0.27 | 27.25 | 27.00 | | | | | |
| | | 60 or | 2 | 0.18 | 1460 | 0.1 | 1.87 | 0.31 | 31.31 | 32.00 | | | | | |
| | | NLt= | 1093 | | 1492 5453 | | 5.97 | 1.00 | | | 0.05 | 0.31 | 0.26 | 0.02 | 10.50 |
| 2 | NDVI | Dead Plant | 307 | 28.0 | 6271 | 42. | 0.67 | 0.21 | 20.68 | 21.00 | | | | | |
| | | Unhealthy | 347 | 31.7 | 3262 | 21. | 1.45 | 0.45 | 44.92 | 45.00 | | | | | |
| | | Healthy | 439 | 40.1 | 5391 | 36. | 1.11 | 0.34 | 34.40 | 34.00 | | | | | |
| | | NLt= | 1093 | | 1492 | | 3.23 | 1.00 | | | 0.21 | 0.45 | 0.24 | 0.02 | 9.72 |
| 3 | Elevation | Less than | 431 | 39.4 | 3685 | 24. | 1.60 | 0.35 | 35.39 | 35.00 | | | | | |
| | | 2000 - 3000 | 299 | 27.3 | 3710 | 24. | 1.10 | 0.24 | 24.39 | 24.00 | | | | | |
| | | 3000 - 4000 | 215 | 19.6 | 2451 | 16. | 1.20 | 0.27 | 26.55 | 27.00 | | | | | |
| | | 4000 - 5000 | 147 | 13.4 | 3298 | 22. | 0.61 | 0.13 | 13.49 | 14.00 | | | | | |
| | | More than | 1 | 0.09 | 1780 | 11. | 0.01 | 0.00 | 0.17 | 0.00 | | | | | |
| | | NLt= | 1093 | | 1492 | | 4.51 | 1.00 | | | 0.00 | 0.35 | 0.35 | 0.02 | 14.12 |
| 4 | Curvature | Upwardly | 542 | 49.5 | 7203 | 48. | 1.03 | 0.35 | 34.75 | 35.00 | | | | | |
| | | Linear (0) | 28 | 2.56 | 4009 | 2.6 | 0.95 | 0.32 | 32.26 | 32.00 | | | | | |
| | | Upwardly | 523 | 47.8 | 7321 | 49. | 0.98 | 0.33 | 32.99 | 33.00 | | | | | |
| | | NLt= | 1093 | | 1492 | | 2.96 | 1.00 | | | 0.32 | 0.35 | 0.02 | 0.02 | 1.00 |
| 5 | Distance from River | Less than | 85 | 7.78 | 7377 | 4.9 | 1.57 | 0.18 | 18.02 | 18.00 | | | | | |
| | | 101-200 m | 120 | 10.9 | 6610 | 4.4 | 2.48 | 0.28 | 28.39 | 28.00 | | | | | |
| | | 201-300 m | 76 | 6.95 | 7110 | 4.7 | 1.46 | 0.17 | 16.72 | 17.00 | | | | | |
| | | 301-400 m | 69 | 6.31 | 6021 | 4.0 | 1.56 | 0.18 | 17.92 | 18.00 | | | | | |
| | | 401-500 m | 39 | 3.57 | 6467 | 4.3 | 0.82 | 0.09 | 9.43 | 9.00 | | | | | |
| | | More than | 704 | 64.4 | 1156 | 77. | 0.83 | 0.10 | 9.52 | 10.00 | | | | | |
| | | NLt= | 1093 | | 1492 | | 8.73 | 1.00 | | | 0.09 | 0.28 | 0.19 | 0.02 | 7.60 |
| 6 | | Less than | 248 | 22.6 | 4547 | 3.0 | 7.45 | 0.56 | 56.11 | 56.00 | | | | | |

| | | | | | | | | | | | | | | | |
|---|---|---|---|---|---|---|---|---|---|---|---|---|---|---|---|
| | Distance from Road | 101-200 m | 26 | 2.38 | 3191 | 2.1 | 1.11 | 0.08 | 8.38 | 8.00 | | | | | |
| | | 201-300 m | 24 | 2.20 | 3115 | 2.0 | 1.05 | 0.08 | 7.93 | 8.00 | | | | | |
| | | 301-400 m | 26 | 2.38 | 2513 | 1.6 | 1.41 | 0.11 | 10.64 | 11.00 | | | | | |
| | | 401-500 m | 28 | 2.56 | 2568 | 1.7 | 1.49 | 0.11 | 11.22 | 11.00 | | | | | |
| | | More than | 741 | 67.8 | 1333 | 89. | 0.76 | 0.06 | 5.72 | 6.00 | | | | | |
| | | NLt= | 1093 | | 1492 | | 13.27 | 1.00 | | | 0.06 | 0.56 | 0.50 | 0.02 | 20.19 |
| 7 | Geology | Archaean | 296 | 27.0 | 4263 | 28. | 0.95 | 0.05 | 5.26 | 5.00 | | | | | |
| | | Mesoproter | 139 | 12.7 | 1602 | 10. | 1.18 | 0.07 | 6.57 | 7.00 | | | | | |
| | | Carbonifero | 18 | 1.65 | 2765 | 1.8 | 0.89 | 0.05 | 4.93 | 5.00 | | | | | |
| | | Neoprotero | 105 | 9.61 | 1573 | 10. | 0.91 | 0.05 | 5.06 | 5.00 | | | | | |
| | | Neoprotero | 1 | 0.09 | 2141 | 1.4 | 0.06 | 0.00 | 0.35 | 0.00 | | | | | |
| | | Permian | 30 | 2.74 | 2215 | 1.4 | 1.85 | 0.10 | 10.26 | 10.00 | | | | | |
| | | Palaeozoic | 34 | 3.11 | 1475 | 9.8 | 0.31 | 0.02 | 1.75 | 2.00 | | | | | |
| | | Proterozoic | 120 | 10.9 | 1031 | 6.9 | 1.59 | 0.09 | 8.81 | 9.00 | | | | | |
| | | Ordovician | 22 | 2.01 | 7824 | 5.2 | 0.38 | 0.02 | 2.13 | 2.00 | | | | | |
| | | Cambrian- | 30 | 2.74 | 5860 | 3.9 | 0.70 | 0.04 | 3.88 | 4.00 | | | | | |
| | | Neoprotero | 196 | 17.9 | 1574 | 10. | 1.70 | 0.09 | 9.43 | 9.00 | | | | | |
| | | Category | Nos. | LSD | Area | Ar | FR | RF | RF% | RF | Min | Max | Max | Min | PR |
| | | Eocene - | 7 | 0.64 | 1568 | 1.0 | 0.61 | 0.03 | 3.38 | 3.00 | | | | | |
| | | Creataceou | 0 | 0.00 | 3988 | 0.0 | 0.00 | 0.00 | 0.00 | 0.00 | | | | | |
| | | Jurassic - | 0 | 0.00 | 4727 | 0.3 | 0.00 | 0.00 | 0.00 | 0.00 | | | | | |
| | | Pliocene - | 3 | 0.27 | 8970 | 0.6 | 0.46 | 0.03 | 2.53 | 3.00 | | | | | |
| | | Palaeoprote | 18 | 1.65 | 4554 | 0.3 | 5.40 | 0.30 | 29.94 | 30.00 | | | | | |
| | | Mesoproter | 74 | 6.77 | 9805 | 6.5 | 1.03 | 0.06 | 5.72 | 6.00 | | | | | |
| | | NLt= | 1093 | | 1492 | | 18.02 | 1.00 | | | 0.00 | 0.30 | 0.30 | 0.02 | 12.00 |
| 8 | LULC | Barren | 132 | 12.0 | 1423 | 9.5 | 1.27 | 0.14 | 13.60 | 14.00 | | | | | |
| | | Waterbody | 14 | 1.28 | 1714 | 1.1 | 1.12 | 0.12 | 11.98 | 12.00 | | | | | |
| | | Forest | 288 | 26.3 | 4166 | 27. | 0.94 | 0.10 | 10.14 | 10.00 | | | | | |
| | | Grass/Grazi | 209 | 19.1 | 1890 | 12. | 1.51 | 0.16 | 16.21 | 16.00 | | | | | |
| | | Builtup | 45 | 4.12 | 2641 | 1.7 | 2.33 | 0.25 | 24.99 | 25.00 | | | | | |
| | | Agriculture | 186 | 17.0 | 2113 | 14. | 1.20 | 0.13 | 12.91 | 13.00 | | | | | |
| | | Barren | 215 | 19.6 | 3209 | 21. | 0.91 | 0.10 | 9.83 | 10.00 | | | | | |
| | | Snow and | 4 | 0.37 | 1685 | 11. | 0.03 | 0.00 | 0.35 | 0.00 | | | | | |
| | | NLt= | 1093 | | 1492 | | 9.31 | 1.00 | | | 0.00 | 0.25 | 0.25 | 0.02 | 9.87 |
| 9 | Geomorphology | Moderately | 255 | 23.3 | 2017 | 13. | 1.73 | 0.02 | 2.13 | 2.00 | | | | | |
| | | Low | 0 | 0.00 | 1154 | 0.0 | 0.00 | 0.00 | 0.00 | 0.00 | | | | | |
| | | Piedmont | 15 | 1.37 | 3523 | 2.3 | 0.58 | 0.01 | 0.72 | 1.00 | | | | | |
| | | Mass | 18 | 1.65 | 4100 | 0.0 | 59.95 | 0.74 | 73.99 | 74.00 | | | | | |
| | | Pediment | 0 | 0.00 | 337 | 0.0 | 0.00 | 0.00 | 0.00 | 0.00 | | | | | |
| | | Alluvial | 10 | 0.91 | 1841 | 1.2 | 0.74 | 0.01 | 0.92 | 1.00 | | | | | |
| | | Flood Plain | 0 | 0.00 | 9952 | 0.0 | 0.00 | 0.00 | 0.00 | 0.00 | | | | | |
| | | Waterbody | 5 | 0.46 | 1525 | 1.0 | 0.45 | 0.01 | 0.55 | 1.00 | | | | | |
| | | Highly | 776 | 71.0 | 9577 | 64. | 1.11 | 0.01 | 1.37 | 1.00 | | | | | |
| | | Dam and | 0 | 0.00 | 549 | 0.0 | 0.00 | 0.00 | 0.00 | 0.00 | | | | | |
| | | Snow | 8 | 0.73 | 2198 | 14. | 0.05 | 0.00 | 0.06 | 0.00 | | | | | |
| | | Glacial | 0 | 0.00 | 6332 | 0.4 | 0.00 | 0.00 | 0.00 | 0.00 | | | | | |
| | | Valley | 0 | 0.00 | 3558 | 2.3 | 0.00 | 0.00 | 0.00 | 0.00 | | | | | |
| | | Glacial | 0 | 0.00 | 1511 | 0.0 | 0.00 | 0.00 | 0.00 | 0.00 | | | | | |
| | | Glacial | 0 | 0.00 | 449 | 0.0 | 0.00 | 0.00 | 0.00 | 0.00 | | | | | |
| | | Anthropoge | 6 | 0.55 | 4989 | 0.0 | 16.42 | 0.20 | 20.27 | 20.00 | | | | | |
| | | Waterbodie | 0 | 0.00 | 40 | 0.0 | 0.00 | 0.00 | 0.00 | 0.00 | | | | | |

| | | | | | | | | | | | | | | | |
|---|---|---|---|---|---|---|---|---|---|---|---|---|---|---|---|
| | | NLt= | 1093 | | 1492 | | 81.03 | 1.00 | | | 0.00 | 0.74 | 0.74 | 0.02 | 29.65 |
| 10 | Soil Type | 3661 | 396 | 36.2 | 4994 | 33. | 1.08 | 0.14 | 14.38 | 14.00 | | | | | |
| | | 3670 | 69 | 6.31 | 7268 | 4.8 | 1.30 | 0.17 | 17.21 | 17.00 | | | | | |
| | | 3671 | 103 | 9.42 | 6087 | 4.0 | 2.31 | 0.31 | 30.68 | 31.00 | | | | | |
| | | 3679 | 137 | 12.5 | 1041 | 6.9 | 1.80 | 0.24 | 23.85 | 24.00 | | | | | |
| | | 3717 | 368 | 33.6 | 5742 | 38. | 0.88 | 0.12 | 11.62 | 12.00 | | | | | |
| | | 6998 | 20 | 1.83 | 1603 | 10. | 0.17 | 0.02 | 2.26 | 2.00 | | | | | |
| | | 11378 | 0 | 0.00 | 3619 | 0.0 | 0.00 | 0.00 | 0.00 | 0.00 | | | | | |
| | | 11730 | 0 | 0.00 | 7738 | 0.5 | 0.00 | 0.00 | 0.00 | 0.00 | | | | | |
| | | 11736 | 0 | 0.00 | 1109 | 0.0 | 0.00 | 0.00 | 0.00 | 0.00 | | | | | |
| | | 11765 | 0 | 0.00 | 1007 | 0.6 | 0.00 | 0.00 | 0.00 | 0.00 | | | | | |
| | | 11930 | 0 | 0.00 | 1505 | 0.1 | 0.00 | 0.00 | 0.00 | 0.00 | | | | | |
| | | NLt= | 1093 | | 1492 | | 7.53 | 1.00 | | | 0.00 | 0.31 | 0.31 | 0.02 | 12.29 |

There are total 1561 landslide locations in the landslide inventory. These locations were divided into two groups i.e Training set(70%) and Test set(30%). There are total 1093 landslide locations in training set and 468 locations in test set. The training set was used to determine FR and subsequent generation of LSM, whereas test set was used to validate the effectiveness of LSM by generating ROC curve, AUC and LD.

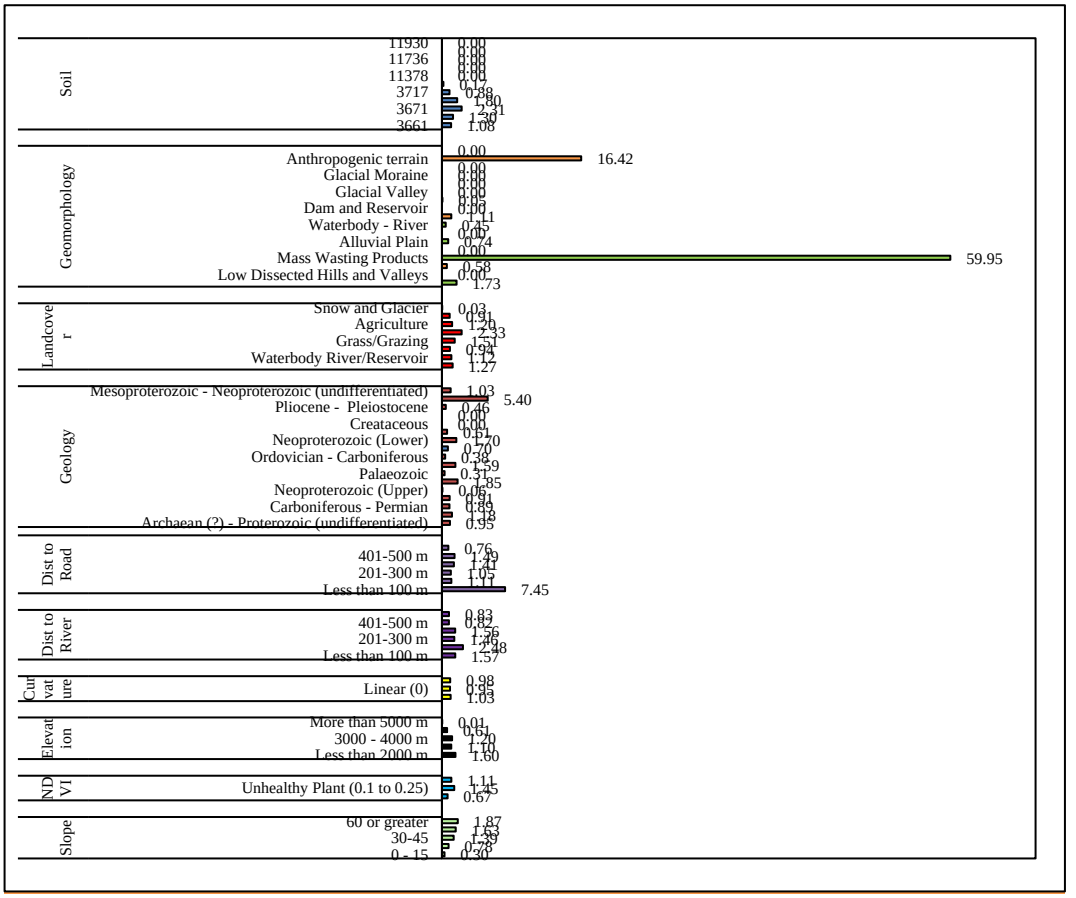


Fig. 5: Frequency Ratio of each class of all factors

As shown in figure no. 5 above, The FR of "Mass Wasting Products" class of Geomorphology layer was found to be maximum i.e. 59.95 amongst all the classes of all factors. It is also noticed that there are many categories of various variables are relatively insignificant to Landslide occurrences. Also, the prediction rate (PR) of Geomorphology was highest i.e.29.64 amongst all the variables which is quite evident from the table 03 given below. This results confirms the importance of Geomorphology feature for landslide occurrences.

Table 03: Prediction Rate of landslide causing factors

| Layer | PR |
|---|---|
| Curvature | 1 |
| Distance from River | 7.59 |
| NDVI | 9.71 |
| LULC | 9.87 |
| Slope | 10.50 |
| Geology | 11.99 |
| Soil Type | 12.29 |
| Elevation | 14.11 |
| Distance from Road | 20.19 |
| Geomorphology | 29.64 |

The construction of the landslide susceptibility map involved the computation and categorization of Landslide Susceptibility Indexes (LSI) across the entire study area. LSI serves as an indicator of the area's susceptibility to landslide occurrences, with smaller values suggesting lower vulnerability. The calculation of LSI relies on the Frequency Ratio (FR) values established during the training process. With the summation of ten factors as shown in below mathematical formula, Landslide susceptibility index map was generated. To create a comprehensive Landslide Susceptibility map, the LSI map was then reclassified into five distinct classes starting from very low to very high as per Jenks Natural Break classification method which is shown below in figure 6.

$$LSI = \sum_{i=1}^{10} PRi * RF_i$$

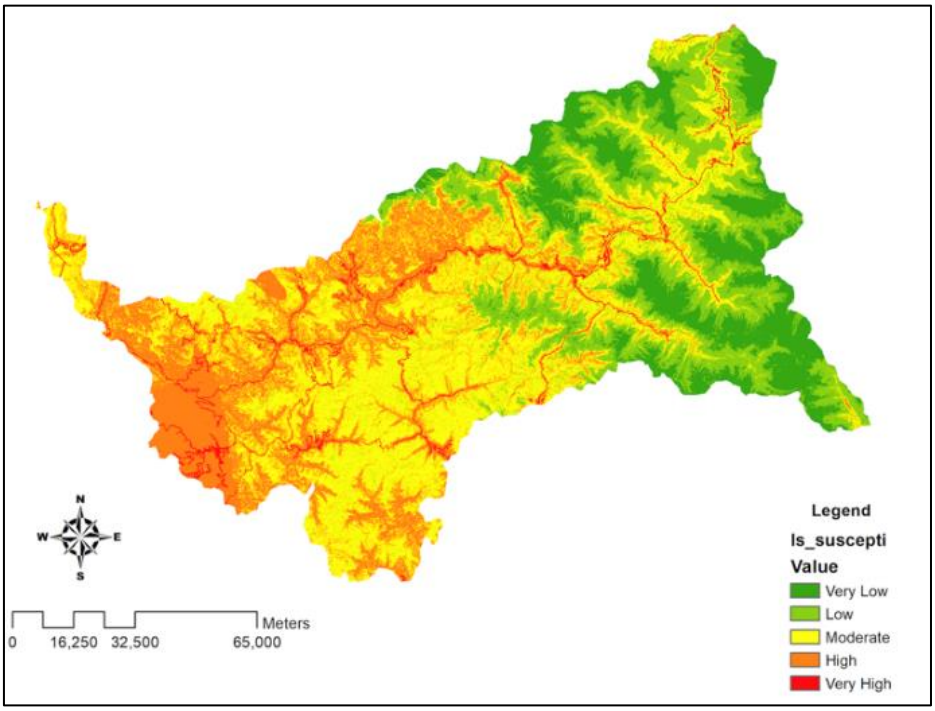


Fig. 6: Landslide Susceptibility Map using FR Approach

Also, the Landslide Density (ratio of number of landslide occurrences and % area of each category) for each category has been determined using remaining 468 landslide locations kept aside as test set which has been shown in the table 4 below. FR modelling produced Maximum Landslide density of 37.31 for "Very High" category of LSM. This value is significantly high when it is compared with correspond values against rest of the categories. This implies that the significant number of landslides fall within relatively small area of "Very High" category of LSM. Also, the gradual increase in the LD values in the last column of the Table.04 can be seen as category becomes from "Very Low" to "Very High". Also, it can be seen that there is only one landslide location is falling in "Very Low" category when tested on test set. This shows the true nature of the prediction surface of LSM.

Table 04: Landslide Density using FR Approach (Training set)

| Sr. No | Category | Nos. Of LSD (NLi) | LSD% | Area (No. Of Pixel) NCi | Area % | Landslide Density |
|---|---|---|---|---|---|---|
| 1 | Very Low | 1 | 0.21 | 2118483 | 14.19 | 0.07 |
| 2 | Low | 46 | 9.83 | 3042120 | 20.38 | 2.26 |
| 3 | Moderate | 146 | 31.20 | 5559024 | 37.25 | 3.92 |
| 4 | High | 160 | 34.19 | 3745741 | 25.10 | 6.38 |
| 5 | Very High | 115 | 24.57 | 460085 | 3.08 | 37.31 |

The final step involves the accuracy evaluation of the Landslide Susceptibility map. This evaluation utilizes landslide inventory data and includes the computation of ROC (Receiver Operating Characteristic) curves and AUC (Area Under the Curve) to validate the effectiveness and reliability of the FR Methodology. The ROC curve for FR modelling has been shown in figure 7 below which resulted in AUC = 0.742.

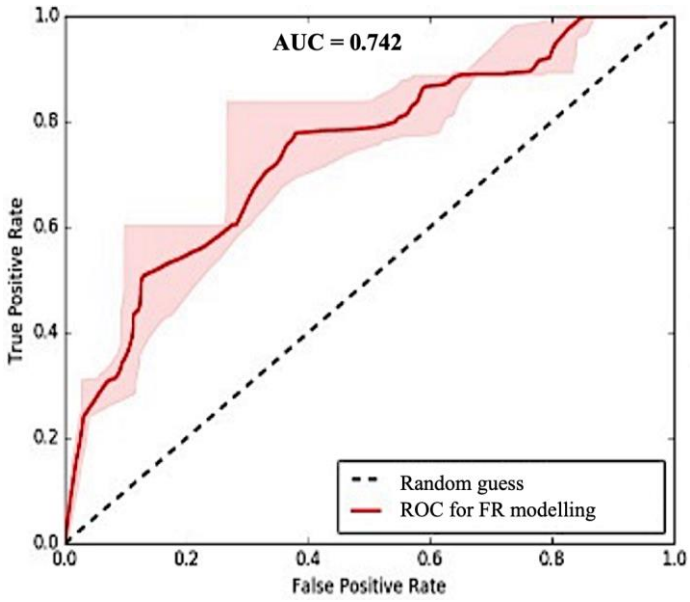


Fig. 7: ROC Curve for FR

Methodology and Analysis using Analytical Hierarchy Process (AHP)

The flow of process involved in AHP approach is shown in the figure 8 below. The methodology and analysis in AHP are divided into 7 different steps which are as discussed below;

1. Pairwise Comparison Matrix: In constructing the pairwise comparison matrix for the Analytical Hierarchy Process (AHP), ten factors including Geomorphology, Distance from Road, Elevation, Soil Type, Geology, Slope, Land Use Land Cover (LULC), NDVI, Distance from River, and Curvature were systematically evaluated using the Saaty scale. This facilitated a thorough analysis of the relative importance and interrelationships among these factors within the decision-making framework. The use of the Saaty scale ensured a consistent and standardized approach to quantify their importance. Table 5 shows the Satty scale in which Intensities of 2, 4, 6, and 8 can be used to express intermediate values. Additionally, intensities such as 1.1, 1.2, 1.3, etc., can be used for elements that are very close in importance. Pairwise comparison matrix showing the relative importance of one variable over the other in the context of Landslide occurrences and corresponding normalised principal Eigen vector (criteria weight) is shown below in figure 9.

Table 05: SATTY Scale for Pairwise Comparisons (Adopted from Satty, 1990)

| Intensity of Importance | Definition | Explanation |
|---|---|---|
| 1 | Equal importance | Two elements contribute equally to the objective |
| 3 | Moderate importance | Experience and judgment moderately favour one element over another |
| 5 | Strong importance | Experience and judgment strongly favour one element over another |
| 7 | Very strong importance | One element is favoured very strongly over another; its dominance is demonstrated in practice |
| 9 | Extreme importance | The evidence favouring one element over another |

| | | |
|---|---|---|
| | | is of the highest possible order of affirmation |

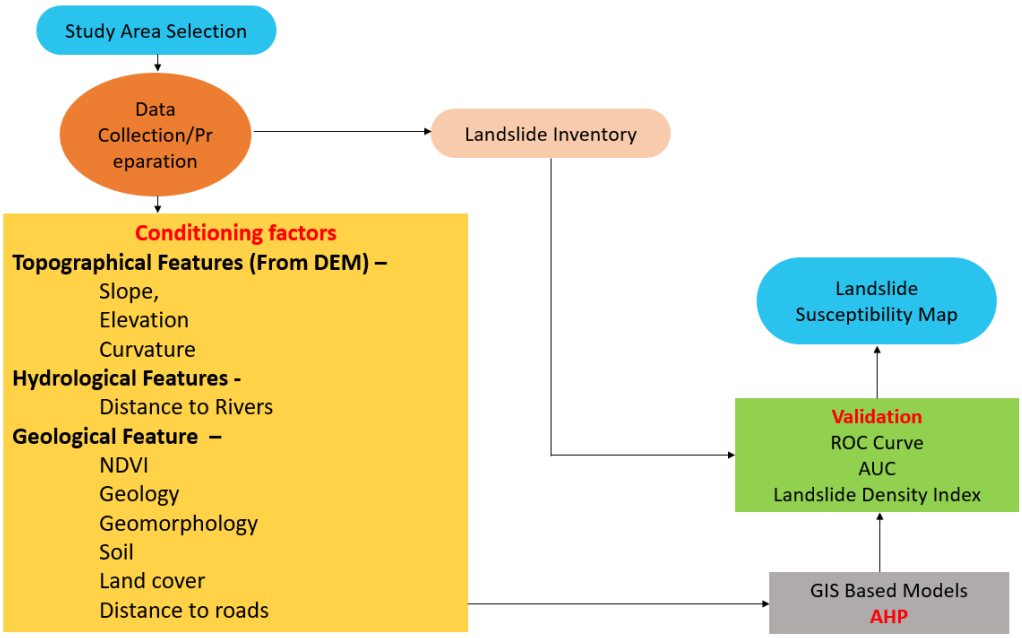


Fig.8: Methodology Process Diagram of AHP

| Matrix | Geomorphology 1 | Distance from Road 2 | Elevation 3 | Soil type 4 | Geology 5 | Slope 6 | LULC 7 | NDVI 8 | Distance from River 9 | Curvature 10 | normalized principal Eigenvector |
|---|---|---|---|---|---|---|---|---|---|---|---|
| Geomorphology 1 | 1 | 2 | 2 | 3 | 3 | 3 | 3 | 3 | 4 | 5 | 22.50% |
| Distance from Road 2 | 1/2 | 1 | 2 | 2 | 2 | 2 | 2 | 2 | 3 | 5 | 15.52% |
| Elevation 3 | 1/2 | 1/2 | 1 | 2 | 2 | 2 | 2 | 2 | 3 | 5 | 13.49% |
| Soil type 4 | 1/3 | 1/2 | 1/2 | 1 | 2 | 2 | 2 | 2 | 2 | 4 | 10.80% |
| Geology 5 | 1/3 | 1/2 | 1/2 | 1/2 | 1 | 2 | 2 | 2 | 2 | 4 | 9.38% |
| Slope 6 | 1/3 | 1/2 | 1/2 | 1/2 | 1/2 | 1 | 1/2 | 2 | 2 | 4 | 7.09% |
| LULC 7 | 1/3 | 1/2 | 1/2 | 1/2 | 1/2 | 2 | 1 | 2 | 2 | 4 | 8.15% |
| NDVI 8 | 1/3 | 1/2 | 1/2 | 1/2 | 1/2 | 1/2 | 1/2 | 1 | 2 | 4 | 6.16% |
| Distance from River 9 | 1/4 | 1/3 | 1/3 | 1/2 | 1/2 | 1/2 | 1/2 | 1/2 | 1 | 3 | 4.56% |
| Curvature 10 | 1/5 | 1/5 | 1/5 | 1/4 | 1/4 | 1/4 | 1/4 | 1/4 | 1/3 | 1 | 2.35% |

Fig.9: Pairwise comparison matrix

2. Normalised Pairwise Comparison Matrix: This matrix standardizes the priorities attributed to each factor, ensuring a balanced and normalized representation of their relative importance in the decision-making process.

3. Determination of Weight Criteria: Normalised value obtain in previous steps are averaged and criteria weight is obtained.

4. Determining Weighted Sum: Weight sum is obtained by multiplying the weight criteria with Pairwise comparison matrix obtained in Step 1. Then the summation of respective values row wise will give the weighted sum.

5. Determining Consistency vector (Ratio): The division of weighted sum and weight criteria gives the consistency vector as shown in Table 6.

Table 06: Determination of Consistency Vector (Ratio)

| Weighted Sum Value | Criteria Weight | Consistency Vector (Ratio) |
|---|---|---|
| 2.36 | 0.22 | 10.58 |
| 1.63 | 0.15 | 10.60 |
| 1.42 | 0.13 | 10.62 |
| 1.14 | 0.11 | 10.65 |
| 0.99 | 0.09 | 10.53 |
| 0.86 | 0.08 | 10.41 |
| 0.75 | 0.07 | 10.31 |
| 0.65 | 0.06 | 10.24 |
| 0.48 | 0.05 | 10.34 |
| 0.25 | 0.02 | 10.32 |

6. Determining Consistency Index and Ratio: In the Analytical Hierarchy Process (AHP), the Consistency Index is calculated by determining the average of the Consistency Vector (Ratio) obtained in the previous step. The Consistency Ratio (CR), essential for evaluating the reliability of the comparisons, is then obtained by dividing the Consistency Index (CI) by its random index counterpart (Random consistency Index(RI)) which is given in table 7 below. Lower values indicate better consistency in the decision-making hierarchy. If the value of CR is less than or equal to 10 percent, the inconsistency amongst the variable relationship is acceptable, but if the CR is greater than 10 percent, the pairwise comparison matrix needs to be revised (Saaty 1977). In the current analysis the value of CR is determined and it is found to be 0.033 which is less than 0.1.

Table 07: Random Constancy Index(RI)

| N | 1 | 2 | 3 | 4 | 5 | 6 | 7 | 8 | 9 | 10 |
|---|---|---|---|---|---|---|---|---|---|---|
| RI | 0 | 0 | 0.58 | 0.9 | 1.12 | 1.24 | 1.32 | 1.41 | 1.45 | 1.51 |

$$CI = \frac{\lambda - n}{n-1}$$

$$CR = \frac{CI}{RI}$$

7. Landslide Susceptibility Index: The obtained weight is then integrated within the causative factors with the equation shown below where $R_i$ is rating class and $W_i$ Weighted index for each of conditioning parameter. Each category of each causative factors were assigned proper weight according to its influence on landslide occurrences. These weights were multiplied by the criteria weight of respective landslide causing factors which were determined in the step 3 above. If was followed by the arithmetic sum of multiples of weight and criteria weight as per the formula shown below and landslide susceptibility index (LSI)

map was prepared. The resulted LSI map is classified into five categories as per Jenks natural breaks classification method which gives five different categories starting from very low to very high and Landslide Susceptibility map is prepared as shown in figure 10 below. Also, the Landslide Density for each category has been determined which has been shown in the table 8 below. AHP produced maximum density of 29.38 for "Very High" category of Landslide susceptibility. Also, It can be seen that 37 landslide locations fall under "Very Low" category of AHP model, whereas in FR model there was only one landslide was falling within the said category.

$$LSI = W_i * \sum_{j=1}^{n} R_j$$

Table 08: Landslide Density using AHP Approach (Training Set)

| Sr. No | Category | Nos. Of LSD (NLi) | LSD% | Area (No. Of Pixel) NCi | Area % | Landslide Density |
|---|---|---|---|---|---|---|
| 1 | Very Low | 37 | 7.91 | 3356286 | 22.49 | 1.65 |
| 2 | Low | 94 | 20.09 | 4736244 | 31.73 | 2.96 |
| 3 | Moderate | 62 | 13.25 | 2563227 | 17.17 | 3.61 |
| 4 | High | 178 | 38.03 | 3776963 | 25.31 | 7.03 |
| 5 | Very High | 97 | 20.73 | 492733 | 3.30 | 29.38 |

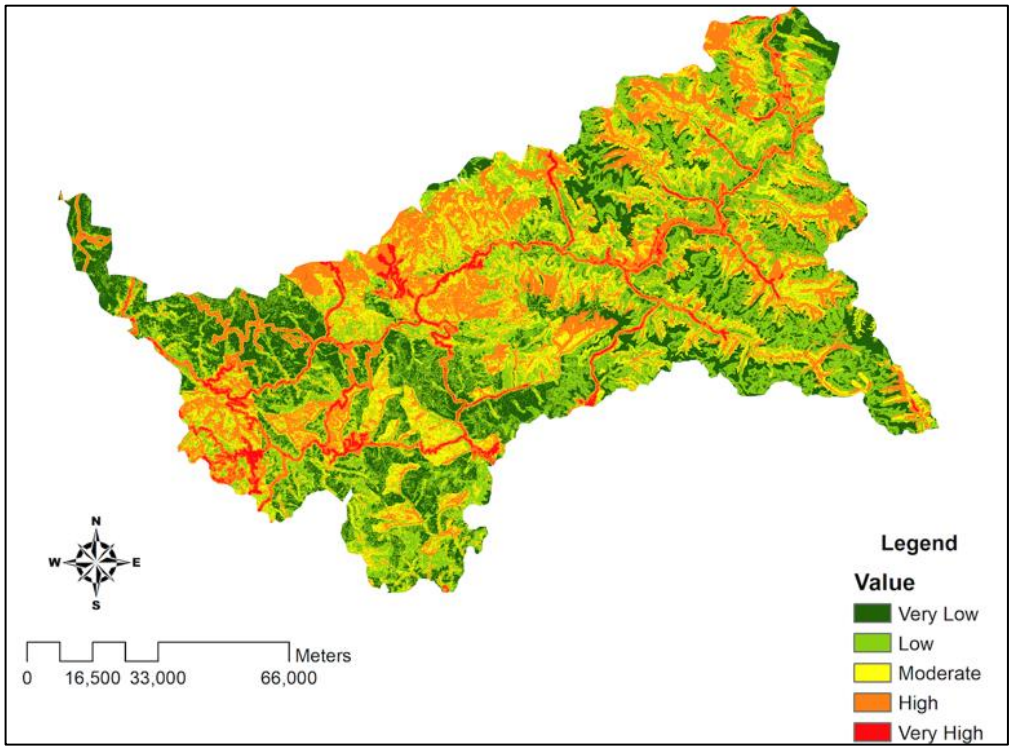


Figure 10: Landslide Susceptibility Map using AHP

Finally, the validation of the effectiveness and reliability of landslide susceptibility modelling

was done by utilizing landslide inventory data and subsequent generation of ROC (Receiver Operating Characteristic) curves and computing AUC (Area Under the Curve). The ROC curve for AHP modelling has been shown in figure 11 below which resulted in AUC = 0.712.

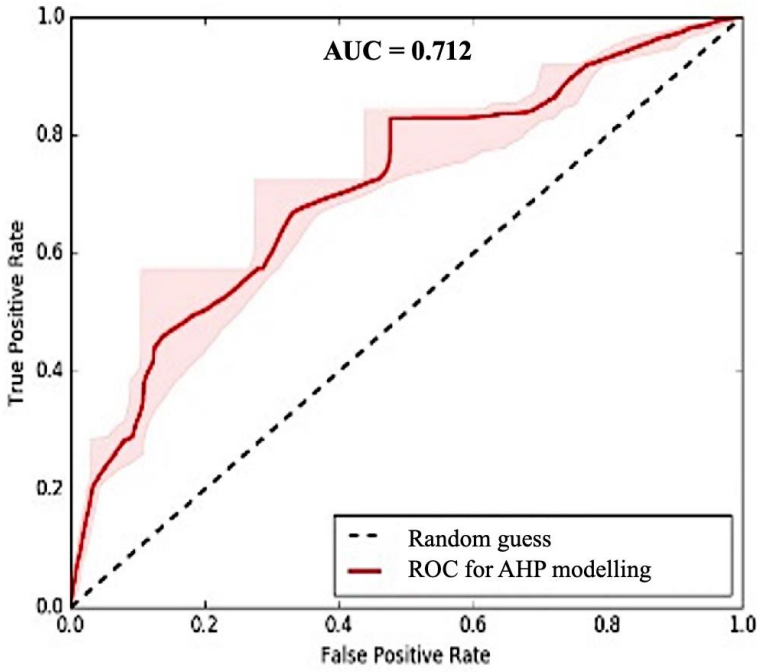


Fig. 11: ROC Curve for AHP

## 6. Results and Discussion

Considering socioeconomic aspect of landslides, the Frequency Ratio (FR) and Analytical Hierarchy Process (AHP) modelling were performed to determine the effectiveness of both the models in determining landslide susceptibility in the lower Sutlej basin, Himachal Pradesh, India. Landslides have the potential to devastate forests, farms, fisheries, industry, communication networks, and drinking water quality [22]. Thus, it is desirable to create a landslide susceptibility map in order to properly develop and manage areas that are prone to landslides. A landslide inventory was created by digitising total of 1561 landslide locations using Google Earth and ArcGIS. In order to assess the spatial association between these characteristics and landslide occurrences, ten landslide conditioning factors (slope, elevation, curvature, NDVI, Soil, landuse, geomorphology, geology, distance to streams and distance to road) were taken into account. Fayez, Laila et al., 2018 used eleven landslide causing factors for LSM and the performance was validated by subsequent quantification of LD. It produced the LD of 1.85 for Very High category.

In this study two quantitative methods were employed to map the landslide susceptibility. The FR method relies on the calculation of Frequency Ratios for different conditioning factors, emphasizing the observed relationships between these factors and landslide occurrences. On the other hand, the AHP method involves a multicriteria decision-making approach,

incorporating expert judgments through pairwise comparisons of various factors to derive their relative importance. The results obtained from the application of FR and AHP reveal variations in the Landslide Susceptibility Index (LSI) across the study area. The Landslide Susceptibility Index (LSI) serves as an indicator of the extent to which an area is prone to landslide occurrences. Areas with smaller LSI values indicate lower susceptibility to landslides, while higher values signify increased vulnerability. A comparative analysis of the two methods demonstrates nuances in their predictive accuracy. Receiver Operating Characteristics curves (ROC) along with Area under the curve (AUC) for both FR and AHP models were derived. Basically, ROC is the plot between True positive rate and False positive rate. Also, higher the value of AUC ($\leq 1$) represents high degree of accuracy of the final LSM. The FR method yields an AUC (Area Under the Curve) value of 0.742 [Fig.7], indicating a satisfactory predictive performance. Conversely, the AHP method produces a slightly lower AUC value of 0.712 [Fig.11]. Further, Landslide Density (LD) for all the categories of both the landslide susceptibility maps were derived using test set data. It can be seen that FR resulted in higher Landslide Density value of 37.31[table 4] for "Very high" category whereas AHP gave lesser density value of 29.38 [table 11] for the same category. Also LD was worked out by considering the entire landslide inventory (1561 landslide locations) for both FR and AHP models[table 09, Fig. 12(a)]. Again, there are more landslides locations are falling in "Very high" category of FR model than AHP model. Also, it can be seen that the number of landslide locations falling in "Very Low" category of FR is significantly less than that in case of AHP [Fig.12(a)]. The LD values for "Low", "Moderate" and "High" categories are almost similar for both FR and AHP models when tested on total inventory [Table 09].

Table 09: Landslide Density for FR and AHP Approach

| Sr. No | Category | Nos. Of LSD (NLi) (FR) | Landslide Density (FR) | Nos. Of LSD (NLi) (AHP) | Landslide Density (AHP) |
|---|---|---|---|---|---|
| 1 | Very Low | 1 | 0.07 | 123 | 5.47 |
| 2 | Low | 172 | 8.44 | 300 | 9.45 |
| 3 | Moderate | 454 | 12.19 | 233 | 13.57 |
| 4 | High | 556 | 22.15 | 593 | 23.43 |
| 5 | Very High | 378 | 122.63 | 312 | 94.51 |

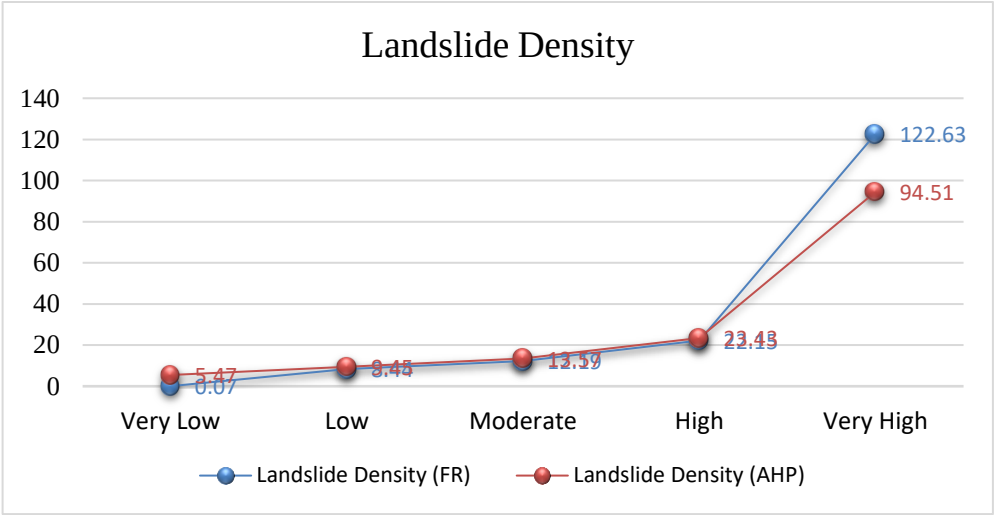


a)

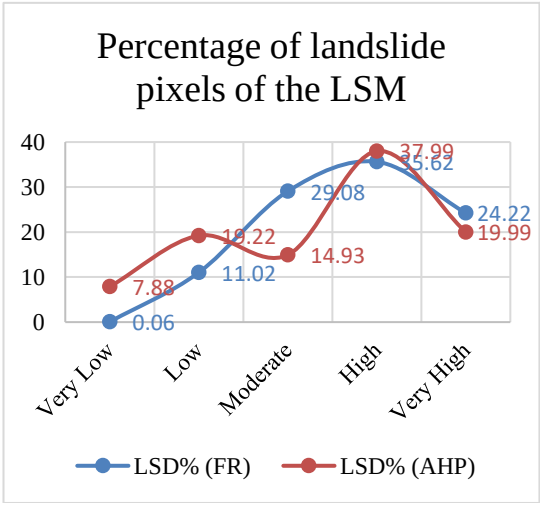


b)

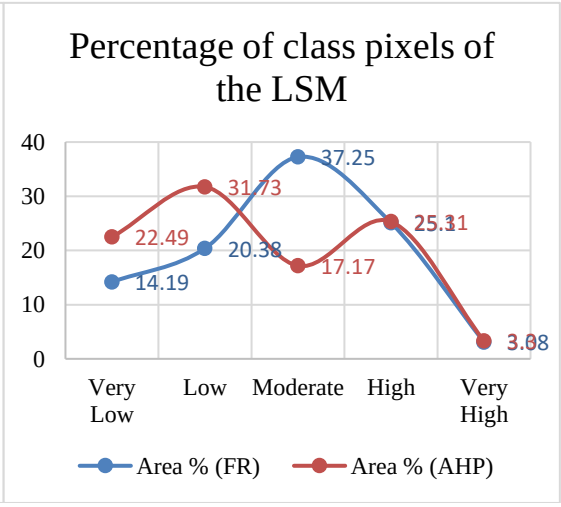


c)

Fig.12: Analysis of FR and AHP on the susceptibility maps: a) FR values of classes of the maps, (b) percentage of landslide pixels of the maps, and (c) percentage of class pixels of the maps

Moreover, the percentage of class pixels [Fig.12b] and percentage of landslide pixels [Fig.12c] of the LSM for both FR and AHP models have been plotted and compared the values for different class of the final susceptibility maps. Looking at the shape of both the curves, It is quite evident that the FR model could classify the index map having less non-linearity, whereas high degree of non-linearity can be seen in AHP model.

Figure 13 below shows the performance of FR and AHP model on different dataset i.e Training, Testing and entire landslide inventory (Training + Testing). One can see the

consistence performance of FR and AHP on all the three dataset. FR performed consistently better than AHP during validation using LD. FR produces consistently high and low value of LD for "Very High" and "Very Low" category respectively when compared to AHP. The performance of both the methods remained consistent when tested using Training, Testing and entire data set. This confirms the absence of overfitting in the LSM in both the classified maps.

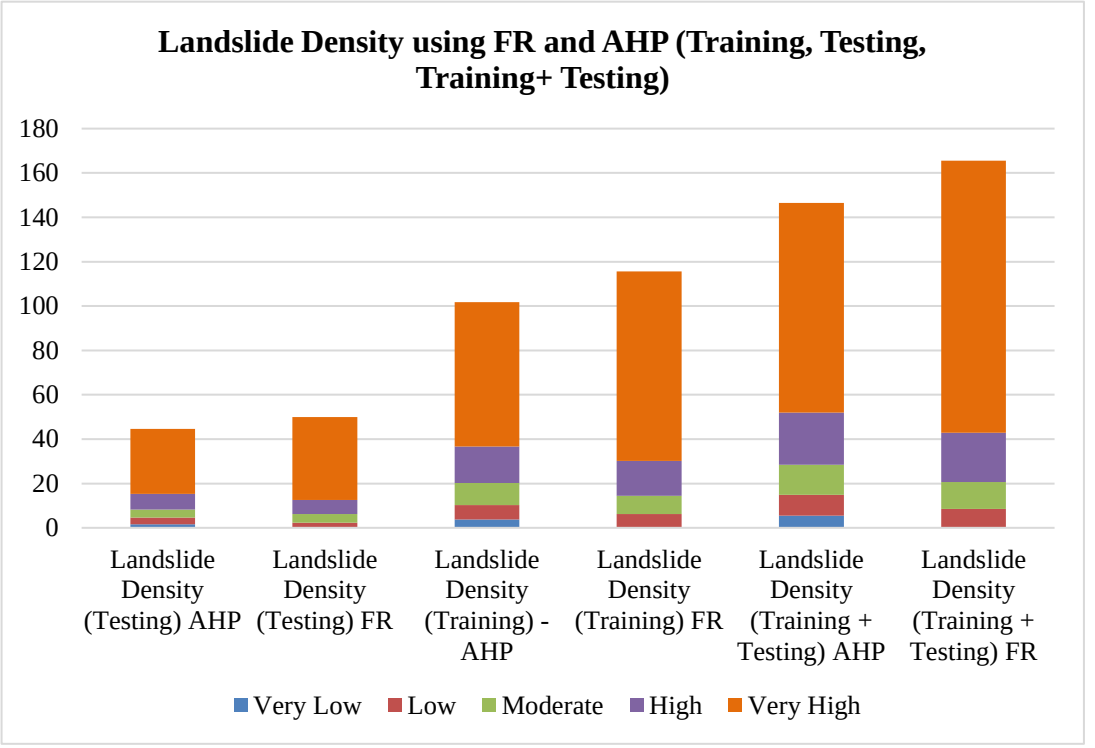


Fig.13: Landslide Density for FR and AHP (Training, Testing, Training + Testing)

The small discrepancy suggests a nuanced difference in the predictive capabilities of the two methods, emphasizing the importance of considering multiple approaches for a comprehensive understanding of landslide susceptibility. The validation process using AUC and LD values serves as a crucial step in assessing the reliability and effectiveness of the developed LSM models.

## 7. Conclusion

This research undertakes a comparison between two prominent methods for Landslide Susceptibility Mapping (LSM) – the Frequency Ratio (FR) and Analytical Hierarchy Process (AHP) using GIS. The study aimed to provide a comprehensive understanding of landslide susceptibility in the Himalayan region, leveraging the statistical robustness of FR and the expert-driven decision-making capability of AHP. The analysis revealed notable differences in the predictive accuracy of the two methods. The FR method exhibited a commendable AUC value of 0.742 and an LD value of 122.63, indicative of strong predictive performance. In

contrast, the AHP method yielded a slightly lower AUC value of 0.712 and an LD value of 94.51. These results demonstrate that the FR method outperforms AHP in terms of predictive accuracy for landslide susceptibility mapping in the study area. While this study offers valuable insights, future research should aim to incorporate dynamic factors, enhance data collection methods, and explore advanced machine learning techniques to further improve the accuracy and robustness of LSM.

## References

1. Kanungo, D. P., Arora, M., & Sarkar, S. (2009). Landslide Susceptibility Zonation (LSZ) Mapping-A Review. www.em-dat.net
2. Dahal, R. K., Hasegawa, S., Nonomura, A., Yamanaka, M., Masuda, T., & Nishino, K. (2008). GIS-based weights-of-evidence modelling of rainfall-induced landslides in small catchments for landslide susceptibility mapping. Environmental Geology, 54(2), 311–324. https://doi.org/10.1007/s00254-007-0818-3.
3. Dai, F. C., Lee, C. F., Li, J., & Xu, Z. W. (2001). Assessment of landslide susceptibility on the natural terrain of Lantau Island, Hong Kong. In Cases and solutions Environmental Geology (Vol. 40, Issue 3). Springer-Verlag.
4. Ercanoglu, M., & Gokceoglu, C. (2002). Assessment of landslide susceptibility for a landslide-prone area (north of Yenice, NW Turkey) by fuzzy approach. Environmental Geology, 41(6), 720–730. https://doi.org/10.1007/s00254-001-0454-2
5. Karnawati, D., Fathani, T. F., Ignatius, S., Andayani, B., Legono, D., & Burton, P. W. (2011). Landslide hazard and community-based risk reduction effort in Karanganyar and the surrounding area, central Java, Indonesia. Journal of Mountain Science, 8(2), 149–153. https://doi.org/10.1007/s11629-011-2107-6
6. Lee, S. (2005). Application of logistic regression model and its validation for landslide susceptibility mapping using GIS and remote sensing data. International Journal of Remote Sensing, 26(7), 1477–1491. https://doi.org/10.1080/01431160412331331012
7. Lee, S., & Min, K. (2001). Statistical analysis of landslide susceptibility at Yongin, Korea. Environmental Geology, 40(9), 1095–1113. https://doi.org/10.1007/s002540100310
8. Pradhan, B. (2010). Remote sensing and GIS-based landslide hazard analysis and cross-validation using multivariate logistic regression model on three test areas in Malaysia. Advances in Space Research, 45(10), 1244–1256. https://doi.org/10.1016/j.asr.2010.01.006
9. Pradhan, B., Chaudhari, A., Adinarayana, J., & Buchroithner, M. F. (2012). Soil erosion assessment and its correlation with landslide events using remote sensing data and GIS: A case study at Penang Island, Malaysia. Environmental Monitoring and Assessment, 184(2), 715–727. https://doi.org/10.1007/s10661-011-1996-8
10. Sarkar, S., & Anbalagan, R. (2008). Landslide hazard zonation mapping and comparative analysis of hazard zonation maps. Journal of Mountain Science, 5(3), 232–240. https://doi.org/10.1007/s11629-008-0172-2
11. Van Westen, C. J. (1997). Statistical landslide hazard analysis. van Westen, C. J., Castellanos, E., & Kuriakose, S. L. (2008). Spatial data for landslide susceptibility, hazard, and vulnerability assessment: An overview. Engineering Geology, 102(3–4), 112–131. https://doi.org/10.1016/j.enggeo.2008.03.010
12. Sarkar, S., Kanungo, D. P., Patra, A. K., & Kumar, P. (2008). GIS based spatial data analysis for landslide susceptibility mapping. Journal of Mountain Science, 5(1), 52–62. https://doi.org/10.1007/s11629-008-0052-9
13. García-Rodríguez, M. J., Malpica, J. A., Benito, B., & Díaz, M. (2008). Susceptibility assessment of earthquake-triggered landslides in El Salvador using logistic regression.

Geomorphology, 95(3–4), 172–191. https://doi.org/10.1016/j.geomorph.2007.06.001

14. Kanungo, D. P., Arora, M. K., Sarkar, S., & Gupta, R. P. (2006). A comparative study of conventional, ANN black box, fuzzy and combined neural and fuzzy weighting procedures for landslide susceptibility zonation in Darjeeling Himalayas. Engineering Geology, 85(3–4), 347–366. https://doi.org/10.1016/j.enggeo.2006.03.004
15. Kim, D., Im, S., Lee, S. H., Hong, Y., & Cha, K. S. (2010). Predicting the rainfall-triggered landslides in a forested mountain region using TRIGRS model. Journal of Mountain Science, 7(1), 83–91. https://doi.org/10.1007/s11629-010-1072-9
16. Nandi, A., & Shakoor, A. (2010). A GIS-based landslide susceptibility evaluation using bivariate and multivariate statistical analyses. Engineering Geology, 110(1–2), 11–20. https://doi.org/10.1016/j.enggeo.2009.10.001
17. Huang, Y., & Zhao, L. (2018). Review on landslide susceptibility mapping using support vector machines. In Catena (Vol. 165, pp. 520–529). Elsevier B.V. https://doi.org/10.1016/j.catena.2018.03.003
18. Goswami, R., Mitchell, N. C., & Brocklehurst, S. H. (2011). Distribution and causes of landslides in the eastern Peloritani of NE Sicily and western Aspromonte of SW Calabria, Italy. Geomorphology, 132(3–4), 111–122. https://doi.org/10.1016/j.geomorph.2011.04.036
19. Lee, S., & Pradhan, B. (2006). Probabilistic landslide hazards and risk mapping on Penang Island, Malaysia.
20. el jazouli, Aafaf & Barakat, Ahmed & Khellouk, Rida. (2019). GIS-multicriteria evaluation using AHP for landslide susceptibility mapping in Oum Er Rbia high basin (Morocco). Geoenvironmental Disasters. 6. 10.1186/s40677-019-0119-7.
21. Khan, Hawas & Shafique, Muhammad & Khan, Muhammad & Bacha, Alam & Shah, Safeer & Calligaris, Chiara. (2018). Landslide susceptibility assessment using Frequency Ratio, a case study of northern Pakistan. The Egyptian Journal of Remote Sensing and Space Science. 22. 10.1016/j.ejrs.2018.03.004.
22. Fayez, Laila & Pazhman, Dawlat & Phạm, Thai & Dholakia, M & Solanki, Hitesh & Khalid, Maizatul & Prakash, Indra. (2018). Application of Frequency Ratio Model for the Development of Landslide Susceptibility Mapping at Part of Uttarakhand State, India. International Journal of Applied Engineering Research. 13.
23. Yalcin, Ali & Reis, Selçuk & Aydinoglu, Arif & Yomralioglu, Tahsin. (2011). A GIS-based comparative study of frequency ratio, analytical hierarchy process, bivariate statistics and logistics regression methods for landslide susceptibility mapping in Trabzon, NE Turkey. CATENA. 85. 274-287. 10.1016/j.catena.2011.01.014.
24. Mandal, Sujit & Maiti, Ramkrishna. (2013). Integrating the Analytical Hierarchy Process (AHP) and the Frequency Ratio (FR) Model in Landslide Susceptibility Mapping of Shiv-khola Watershed, Darjeeling Himalaya. International Journal of Disaster Risk Science 2095-5970/N. 2013. 200-212. 10.1007/s13753-013-0017-7.
25. Biswas, B., Rahaman, A. & Barman, J. Comparative Assessment of FR and AHP Models for Landslide Susceptibility Mapping for Sikkim, India, and Preparation of Suitable Mitigation Techniques. J Geol Soc India 99, 791–801 (2023). https://doi.org/10.1007/s12594-023-2386-x
26. Pham, B. T., Pradhan, B., Tien Bui, D., Prakash, I., & Dholakia, M. B. (2016). A comparative study of different machine learning methods for landslide susceptibility assessment: A case study of Uttarakhand area (India). Environmental Modelling and Software, 84, 240–250. https://doi.org/10.1016/j.envsoft.2016.07.005
27. Pham, B. T., & Prakash, I. (2019). Evaluation and comparison of LogitBoost Ensemble, Fisher's Linear Discriminant Analysis, logistic regression and support vector machines methods for landslide susceptibility mapping. Geocarto International, 34(3), 316–333. https://doi.org/10.1080/10106049.2017.1404141

28. Pourghasemi, Hamid & Yansari, Zeinab & Panagos, Panos & Pradhan, Biswajeet. (2018). Analysis and evaluation of landslide susceptibility: a review on articles published during 2005–2016 (periods of 2005–2012 and 2013–2016). Arabian Journal of Geosciences. 11. 10.1007/s12517-018-3531-5.
29. Ercanoglu, Murat. (2005). Landslide susceptibility assessment of SE Bartin (West Black Sea region, Turkey) by artificial neural networks. Natural Hazards and Earth System Science. 5. 10.5194/nhess-5-979-2005.
30. Dikshit, Abhirup & Sarkar, Raju & Pradhan, Biswajeet & Segoni, Samuele. (2020). Rainfall Induced Landslide Studies in Indian Himalayan Region: A Critical Review. Applied Sciences. 2020. 2466. 10.3390/app10072466.